



Cite this: *New J. Chem.*, 2016, 40, 5808

C,N-Chelated organotin(IV) azides: synthesis, structure and use within click chemistry†

Petr Švec,^{*a} Karel Bartoš,^b Zdeňka Růžicková,^a Petra Cuřínová,^c Libor Dušek,^d Jan Turek,^e Frank De Proft^e and Aleš Růžička^a

A set of tri- and diorganotin(IV) azides bearing 2-(*N,N*-dimethylaminomethyl)phenyl as a C,N-chelating ligand (L^{CN}) has been prepared and structurally characterized. Triorganotin(IV) azides of the type $L^{CN}R_2SnN_3$ ($R = n\text{-Bu}$ (**1**) and Ph (**2**)) and $(L^{CN})_2(n\text{-Bu})SnN_3$ are monomeric both in solution and in the solid state. The central tin atom in these species is five-coordinated with distorted trigonal bipyramidal geometry. Diorganotin(IV) azides of the type $L^{CN}R_2Sn(N_3)_2$ ($R = n\text{-Bu}$ and Ph) are monomeric with trigonal bipyramidal geometry around the tin atom as well. Finally, $(L^{CN})_2Sn(N_3)_2$ contains a six-coordinated tin atom with heavily distorted octahedral geometry due to the presence of two L^{CN} units. The potential use of selected organotin(IV) azides **1** and **2** as useful building blocks within click chemistry was investigated. The reactions of **1** and **2** with various nitriles resulted in the formation of corresponding triorganotin(IV) tetrazolides (i.e. $\kappa\text{-N}^1$: $L^{CN}(n\text{-Bu})_2Sn(5\text{-MeCN}_4)$, $L^{CN}Ph_2Sn(5\text{-MeCN}_4)$, $L^{CN}(n\text{-Bu})_2Sn(5\text{-Me}_2NCH_2CN_4)$, $L^{CN}Ph_2Sn(5\text{-Me}_2NCH_2CN_4)$; and $\kappa\text{-N}^2$: $L^{CN}(n\text{-Bu})_2Sn(5\text{-}t\text{-BuCN}_4)$, $L^{CN}Ph_2Sn(5\text{-}t\text{-BuCN}_4)$, $L^{CN}(n\text{-Bu})_2Sn(5\text{-PhCN}_4)$, $L^{CN}Ph_2Sn(5\text{-PhCN}_4)$). Similarly, the reaction of **1** and **2** with cyclooctyne provided corresponding C,N-chelated di-*n*-butyl/diphenyltin(IV) $\kappa\text{-N}^1$ 4,5,6,7,8,9-hexahydrocycloocta[*d*][1,2,3]triazol-1-ides. All azido complexes and products of the [3+2] cycloaddition reactions were characterized by the combination of elemental analysis, mass spectrometry, IR spectroscopy, multinuclear NMR spectroscopy and, in the case of crystalline materials, XRD analysis. In addition, DFT calculations were carried out within the click chemistry reactions in order to corroborate the preferred formation of the respective tetrazolide regioisomer.

Received (in Victoria, Australia)
12th November 2015,
Accepted 28th February 2016

DOI: 10.1039/c5nj03187g

www.rsc.org/njc

1. Introduction

The first organotin(IV) azides were prepared conveniently in the 1960s (i) by the reaction of organotin(IV) chlorides with NaN_3 ¹ or (ii) by the reaction of organotin(IV) amines with HN_3 .² In the solid state, these species have mainly polymeric structures *via* bridging azide groups. The majority of polymeric organotin(IV)

azides (Fig. 1A) reveal a distorted trigonal bipyramidal geometry around the central tin atom (e.g. Me_3SnN_3 ,³ Ph_3SnN_3 ,⁴ Bn_3SnN_3 ⁵ or $(\text{Cy}_3\text{Sn})_2\text{N}_3(\text{OH})$ ⁶). Organotin(IV) azides, usually bearing bulky (organic) substituents, behave as monomeric species with tetrahedrally coordinated tin centers as demonstrated, for example, for $(t\text{-Bu})_3\text{SnN}_3$ and $(t\text{-Bu})_2\text{Sn}(\text{N}_3)_2$ ⁷ or $(\text{Neo})_3\text{SnN}_3$.⁸ The presumed polymerization of (organo)tin(IV) azides may also be prevented by the formation of adducts with ligands containing donor atoms (such as O and N) as shown for $\text{Ph}_3\text{SnN}_3 \cdot \text{L}$ ($\text{L} = \text{HMPA}$, $\text{Ph}_3\text{P}=\text{O}$, pyridine, etc.), $\text{Sn}(\text{N}_3)_4 \cdot 2\text{py}$ or $\text{Sn}(\text{N}_3)_4 \cdot \text{bipy}$ ⁴ or by the incorporation of chelating ligand(s) within the molecule. The reactivity of

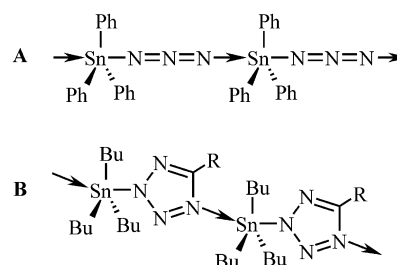


Fig. 1 Structural drawings of polymeric triorganotin(IV) azide (A) and tetrazolide (B; $\text{Bu} = n\text{-Bu}$, $\text{R} = (\text{CH}_2)_n\text{SnR}_3$).

^a Department of General and Inorganic Chemistry, Faculty of Chemical Technology, University of Pardubice, Studentská 573, CZ-532 10, Pardubice, Czech Republic.

E-mail: petr.svec2@upce.cz

^b High School of Chemistry Pardubice, Poděbradská 94, CZ-530 09, Pardubice, Czech Republic

^c Department of Analytical and Material Chemistry, Institute of Chemical Process Fundamentals, Czech Academy of Sciences, v.v.i., Rozvojová 135/1, CZ-165 02, Prague, Czech Republic

^d Institute of Environmental and Chemical Engineering, Faculty of Chemical Technology, University of Pardubice, Studentská 573, CZ-532 10, Pardubice, Czech Republic

^e Eenheid Algemene Chemie (ALGC), Member of the QCMM VUB-UGent Alliance Research Group, Vrije Universiteit Brussel, Pleinlaan 2, 1050 Brussels, Belgium

† Electronic supplementary information (ESI) available: All synthetic details, selected NMR and crystallographic parameters and additional figures of molecular structures as well as the computational details with optimized structures. CCDC 1432629–1432635 numbers for compounds **2**, **4**, **6**, **8**, **10**, **11** and **14a**. For ESI and crystallographic data in CIF or other electronic format see DOI: 10.1039/c5nj03187g



some stannylenes (tin(II) complexes) towards Me_3SiN_3 has been studied from an experimental⁹ as well as theoretical point of view.^{9c,10} We have recently described the solution behaviour and solid state structures of two monomeric tin(IV) azides bearing either chelating or bulky bis(trimethylsilyl)amido ligands. These species were obtained by the oxidation of the corresponding stannylene with Me_3SiN_3 .^{9c}

In contrast, the family of tin(II) compounds bearing the azide moiety is known to a lesser extent. These species involve, for example, $[(\text{Mes})_2\text{DAP}]\text{SnN}_3$ (DAP = diazapentadienyl),¹¹ $[(n\text{-Pr})_2\text{ATI}]\text{SnN}_3$ (ATI = aminotroponimate)¹² or $[\text{HB}(3,5\text{-(CF}_3)_2\text{-Pz})_3]\text{AgSn}(\text{N}_3)[(n\text{-Pr})_2\text{ATI}]$ ($[\text{HB}(3,5\text{-(CF}_3)_2\text{-Pz})_3]$ = hydrotris(3,5-bis(trifluoromethyl)pyrazolyl)borate)¹³ described by Dias and co-workers.

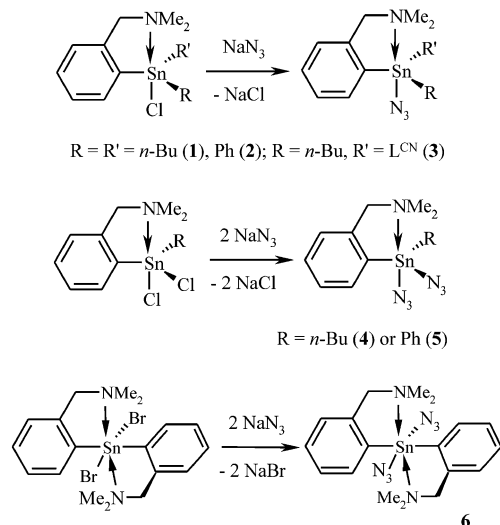
The term “click chemistry” was coined by Sharpless in 2001¹⁴ and this area of chemistry is undergoing an exponential growth because of its benefits.¹⁵ In fact, the well-known 1,3-dipolar azide–alkyne Huisgen cycloaddition can be considered as the first described “click reaction”.¹⁶ The aspects of click chemistry reactions have been investigated by theoretical methods as well.¹⁷ To the best of our knowledge, the possible use of organotin(IV) azides in the [3+2] cycloaddition reaction with a nitrile was first described by Sisido *et al.* in 1971. The first *N*-trialkyltin(IV)-5-substituted tetrazoles were thus prepared.¹⁸ This chemistry has been further expanded mainly by Molloy¹⁹ who described the formation of oligomers,^{19c} linear polymers^{19b} (Fig. 1B) or layered supramolecular arrays^{19c} constituted of the triorganotin(IV) tetrazolide units.

The incorporation of a C,N-chelating ligand within a class of (organo)tin(IV) compounds gives rise to an intramolecular interaction between tin and nitrogen (*i.e.* the $\text{N} \rightarrow \text{Sn}$ coordination). As a consequence of this effect, these species usually tend to form monomeric molecular structures with mainly five- or six-coordinated tin centers.^{20,21} Synthesis, structural studies as well as possible applications of a plethora of C,N-chelated organotin(IV) halides and pseudohalides containing the 2-(*N,N*-dimethylaminomethyl)phenyl ligand have been reported up to now.^{22–28} In this paper, we report on the expansion of the family of known monomeric tri- and diorganotin(IV) azides and their ability to undergo the [3+2] cycloaddition with nitriles or alkynes.

2. Results and discussion

2.1 Synthesis and general remarks

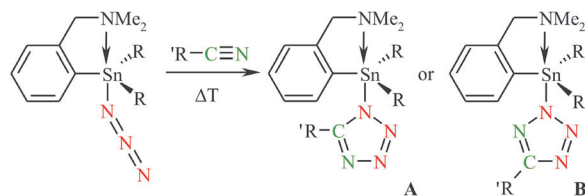
Six novel C,N-chelated organotin(IV) azides [*i.e.* $\text{L}^{\text{CN}}(n\text{-Bu})_2\text{SnN}_3$ (**1**), $\text{L}^{\text{CN}}\text{Ph}_2\text{SnN}_3$ (**2**), $(\text{L}^{\text{CN}})_2(n\text{-Bu})\text{SnN}_3$ (**3**), $\text{L}^{\text{CN}}(n\text{-Bu})\text{Sn}(\text{N}_3)_2$ (**4**), $\text{L}^{\text{CN}}\text{PhSn}(\text{N}_3)_2$ (**5**) and $(\text{L}^{\text{CN}})_2\text{Sn}(\text{N}_3)_2$ (**6**)] were prepared by the reaction of the corresponding C,N-chelated organotin(IV) halides with an excess of sodium azide in the water/diethyl ether (or water/dichloromethane, respectively) mixture (Scheme 1). Compounds **1–6** do not hydrolyze in moist air and are exceptionally stable species. Thus, for example, the hexane solution of **1** can be irradiated with UV light (253.7 nm) overnight in the air without decomposition. Furthermore, **1** is thermally robust,



Scheme 1 Preparation of C,N-chelated organotin(IV) azides **1–6**. Reactions are carried out in a water/diethyl ether (valid for **1**, **3** and **4**) or a water/dichloromethane (valid for **2**, **5** and **6**) mixture of solvents.

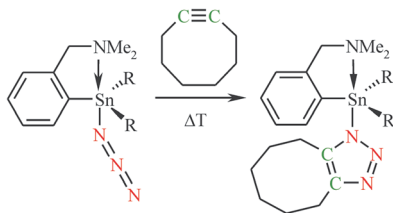
showing no signs of dinitrogen liberation upon heating up to 300 °C for one hour. On the other hand, these organotin(IV) azides react with hydrochloric acid to give corresponding organotin(IV) chlorides and hydrazoic acid as a volatile by-product. In general, the organotin(IV) pseudohalides bearing *n*-Bu substituent(s) could be isolated in higher yields (up to 85% in the case of **1**), while the presence of the phenyl substituents or the second L^{CN} moiety led to a significant decrease of the isolated yield (*e.g.* only 51% in the case of **6**). A possible explanation is that the species bearing the *n*-Bu substituent(s) are easier to extract from the heterogeneous reaction mixture. Unfortunately, the attempted synthesis of the proposed C,N-chelated tin(IV) tris(azide) $\text{L}^{\text{CN}}\text{Sn}(\text{N}_3)_3$ resulted in the formation of a mixture of several inseparable tin-containing compounds.

The reactivity of prepared organotin(IV) azides **1** and **2** towards species containing either the $\text{C}\equiv\text{N}$ or the $\text{C}\equiv\text{C}$ bond (Schemes 2 and 3) has been studied within the scope of click chemistry. It is a well-known fact that the course of a click chemistry reaction can be promoted by addition of a Cu(I) catalyst²⁹ or by heating up the reaction mixture.³⁰ According to our findings, surprisingly, none of the studied click reactions could be promoted by the Cu(I) catalyst (*i.e.* CuI, a mixture of CuSO_4 and sodium ascorbate,



Scheme 2 Preparation of C,N-chelated organotin(IV) tetrazolides **7–14** (for $\text{R} = n\text{-Bu}$: $\text{R} = \text{Me}$ (**7**), *t*-Bu (**9**), Ph (**11**), Me_2NCH_2 (**13**); for $\text{R} = \text{Ph}$: $\text{R} = \text{Me}$ (**8**), *t*-Bu (**10**), Ph (**12**), Me_2NCH_2 (**14**)). A = C,N-chelated organotin(IV) 5-*R*-tetrazol-1-ide regioisomer; B = C,N-chelated organotin(IV) 5-*R*-tetrazol-2-ide regioisomer.





Scheme 3 Preparation of C,N-chelated organotin(IV) triazolides **15** (R = *n*-Bu) and **16** (R = Ph).

and [NHC]CuBr³¹ were tested for this purpose). Therefore, all click chemistry experiments had to be performed at elevated temperatures, similar to those described in the literature.¹⁹ Depending on the boiling point of the reagent employed, either an excess or a strictly stoichiometric amount of organic nitrile or cyclooctyne was used. The corresponding products (*i.e.* organotin(IV) tetrazolides **7–14** and organotin(IV) triazolides **15–16**) were prepared by the [3+2] cycloaddition reactions in essentially quantitative yields and sufficient purity. On the other hand, prolonged reaction times were required (starting from two days in the case of **15** and **16** up to twenty days in the case of **13**) when compared with literature reports.¹⁹ Such extremely long reaction times were required, for example, for the preparation of 1,4-disubstituted Δ^2 -tetrazolin-5-ones.³² All reactions, except for the synthesis of **13** and **14**, could be carried out in the air. When trying to crystallize species **14** from a chloroform solution, acidolysis (due to the action of the hydrochloric acid present in the solvent) occurred providing several single crystals of the corresponding 5-*N,N*-dimethylaminomethyl-1*H*-tetrazole **14a** which were characterized by XRD analysis (see Fig. S4 and S5 in the ESI†). L^{CN}Ph₂SnCl was further identified as a side product by multinuclear NMR spectroscopy in the solution.

As discussed above, cyclooctyne proved to be more reactive in the studied click reactions than organic nitriles. On the other hand, when linear acetylenes (*i.e.* PhC≡CPh, MeC≡CMe and PhC≡CH, respectively) were used instead of cyclooctyne, the formation of the target organotin(IV) triazolides, even when the reaction mixtures were heated to reflux for one week, was not observed. These reactivity issues were also investigated from a theoretical point of view (*vide infra*). In principle, the considered click chemistry reactions may result in the formation of a mixture of tetrazolide regioisomers as demonstrated in Scheme 2. Fortunately, exclusive formation of organotin(IV) 5-*R*-tetrazol-1-ides **7**, **8**, **13** and **14** was observed when a small (Me) or flexible (Me₂NCH₂) substituent was bound to the nitrile moiety. As one would expect, organotin(IV) 5-*R*-tetrazol-2-ide regioisomers **9–12** were formed when nitriles bearing more bulky organic groups (*t*-Bu and Ph) were employed. These findings were the basis of additional DFT calculations (*vide infra*).

2.2 Spectroscopic studies

All ¹H NMR spectra of **1–6** were recorded in CDCl₃ (see Scheme S1, ESI† for the NMR numbering). Furthermore, in some cases (**1** and **2**), the NMR measurements were performed again in benzene-*d*₆ in order to improve the differentiation of resonances

in the aromatic region of the spectra. Both multiplicity and integral intensities of signals are in perfect accordance with presumed structures. The resonances of aromatic protons (H(6)) are accompanied by the characteristic tin satellites with reasonable ^{117/119}Sn–¹H coupling constants (see Table S1 and detailed NMR characterization in the ESI†). In principle, diorganotin(IV) bis(azides) exhibit larger coupling constants (³J(¹¹⁹Sn, ¹H) values that vary from 84 Hz for **4** to 102 Hz for **6**, respectively) than the triorganotin(IV) azides (ranging from 64 Hz for **1** to 73 Hz in case of **2**) which is in good agreement with previously published results.^{22–28,33} The ¹H NMR spectrum of **6** bearing two L^{CN} substituents reveals an AX spin pattern at 3.77 and 3.49 ppm (Δδ = 142 Hz, ²J(¹H, ¹H) = 14 Hz) due to the CH₂N fragments which is a typical phenomenon for this family of compounds.^{24,28}

The ¹H NMR spectra of compounds **7–16** measured in CDCl₃ are quite similar to the spectra of the corresponding **1** and **2** exhibiting additional resonances due to the R substituent originating from the organic nitrile or cyclooctyne.

The presence of the desired species was detected in the ¹³C NMR spectra of **1–16** recorded in CDCl₃. All relevant carbon resonances of L^{CN} and *n*-Bu or Ph substituents are accompanied by tin satellites (see Table S1 and detailed NMR characterization in the ESI†). As discussed above for the ¹H NMR spectra, significantly larger ¹J(^{119/117}Sn, ¹³C) coupling constants are observed for the diorganotin(IV) azides **4–6** than for the triorganotin(IV) ones (**1–3**) which is in accordance with previously published data.^{22–28,33} Species **7–16** further exhibit resonances of the corresponding alkyl/aryl substituents (Me, Ph, *t*-Bu and Me₂NCH₂, respectively) or the C₈ rings at reasonable regions of the carbon NMR spectra.

The formation of the respective tetrazolide ring of **7–14** is confirmed by the presence of a resonance found at higher frequencies (ranging from 158.1 ppm for **8** to 172.4 ppm in the case of **10**) when compared to the signal of the starting organic nitrile (C≡N fragment at *ca.* 110–125 ppm).³⁴ Similarly, a broad signal of the triazolide rings at 144.8 and 144.1 ppm is observed in the case of **15** and **16**, respectively, along with the disappearance of the corresponding signal of the starting cyclooctyne (*ca.* 95 ppm).

The ¹¹⁹Sn NMR spectra of **1–6** measured in CDCl₃ exhibit only one resonance significantly shifted to lower frequencies with respect to the starting C,N-chelated organotin(IV) halides (Table S1, ESI†). The same trend was described recently for other structurally related organotin(IV) pseudohalides bearing the C,N-chelating ligand.²⁸ From another point of view and based on previous results,^{22–28,33} we assume that all organotin(IV) azides **1–6** are monomeric in solution. Owing to the presence of the C,N-chelating ligand(s), the central tin atom in compounds **1–5** is five-coordinate with a distorted trigonal bipyramidal geometry. In spite of the presence of two C,N-chelating ligands in the case of **3**, we assume that only one of them is involved in the intramolecular N→Sn coordination and the presumed equilibrium between coordinated and non-coordinated bonding modes is too fast to be seen on the relatively slow NMR time scale. On the other hand, the central tin atom in monomeric **6** is clearly six-coordinate due to the presence of two C,N-chelating ligands



that are both involved in the intramolecular N→Sn interaction. This hypothesis is based on the recorded ^{119}Sn chemical shift value (−312.6 ppm). The resonance is shifted highly upfield when compared to the corresponding $(\text{L}^{\text{CN}})_2\text{SnCl}_2$ ($\delta(^{119}\text{Sn}) = -252.8$ ppm) or $(\text{L}^{\text{CN}})_2\text{SnBr}_2$ ($\delta(^{119}\text{Sn}) = -271.2$ ppm) where the tin atom is also six-coordinated.²⁴ Generally, the coordination number of the tin atom does not increase upon the addition of a potentially coordinating solvent (THF- d_8) since the ^{119}Sn NMR chemical shift values differ only by a few ppm when compared to values recorded in CDCl_3 (see the ESI†, Experimental part for **1** and **2**).

The ^{119}Sn chemical shift values of monomeric **7–16** are shifted more or less to lower frequencies with respect to the corresponding C,N-chelated organotin(IV) azides **1** and **2** (Table S1, ESI†). Based on these values we assume that the central tin atom remains five-coordinated in all cases.

Low temperature NMR measurements of **8** were carried out in order to investigate its potential isomerisation (Scheme 2). Two signals were observed in the ^{119}Sn NMR spectrum (−217.7 and −223.4 ppm) at −40 °C (as the lowest temperature due to solubility reasons) in the mutual ratio of 1:10. Unfortunately, this phenomenon is not visible in the ^1H and ^{13}C NMR spectra. This could be connected to the fact that two isomers probably coexist at low temperature, while the stable one is observable as a sole species at room temperature with the ^1H and ^{13}C NMR spectra being insensitive to that process.

The infrared spectra of novel organotin(IV) azides **1–6** reveal very strong bands in the range of 2050 cm^{-1} (**2**) to 2066 cm^{-1} (**4**) which are characteristic for the $\nu(\text{N}=\text{N}=\text{N})$ stretching vibration. These bands diminish upon the formation of the tetrazolide or triazolide ring. All assignments were in good agreement with the literature.³⁵

Similarly to the MS spectral patterns of starting chlorides or related carboxylates,³⁶ where the most intense isotopic clusters correspond to the formation of $[\text{M}-\text{X}]^+$ (X = halide or carboxy group) particles as a result of the disconnection of the most labile bond, the measured HR ESI-MS spectra of **1–6** usually provide the $[\text{M}-\text{N}_3]^+$ peaks (100% intensity, see the ESI† page S19) with characteristic isotopic tin cluster in the positive ion mode. The $[\text{M}+\text{Na}]^+$ ions are also observed but with a significantly lower intensity along with other minor particles. The MS spectra of **7**, **8**, **10** and **11** did not provide relevant structural data about the formation or stability of relevant regioisomers of organotin(IV) tetrazolides.

2.3 Solid state structural studies

The molecular structures of **2**, **4**, **6**, **8**, **10**, **11** and **14a** have been established using single-crystal XRD techniques. Suitable single crystals were obtained from the corresponding chloroform or dichloromethane solution by slow evaporation of the solvent in the air.

2.3.1 Molecular structures of 2, 4 and 6. The vicinity of the central tin atom in monomeric **2** adopts a distorted trigonal bipyramidal geometry (Fig. 2). Owing to Bent's rule,³⁷ both the electronegative atom N and the azide moiety occupy axial positions and all three carbon atoms originating from the presence

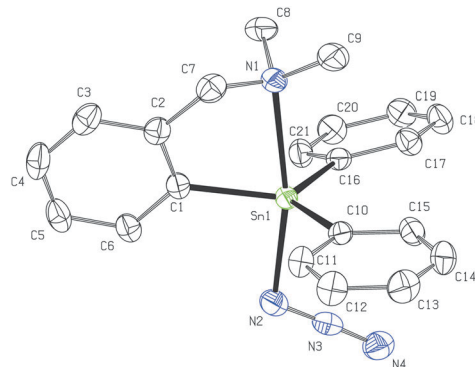


Fig. 2 Molecular structure of **2** (ORTEP presentation, 50% probability level). Hydrogen atoms are omitted for clarity. Selected interatomic distances [Å] and angles [°]: Sn1–N1 2.4590(19), Sn1–N2 2.2298(19), N2–N3 1.194(3), N3–N4 1.150(3), Sn1–C1 2.1140(19), Sn1–C10 2.1222(19), Sn1–C16 2.1269(19); N1–Sn1–N2 168.03(6), Sn1–N2–N3 111.22(14), N2–N3–N4 178.0(2), C1–Sn1–C10 115.44(7), C1–Sn1–C16 121.46(7), C10–Sn1–C16 122.09(7).

of L^{CN} and Ph substituents are situated in the equatorial plane. The N→Sn intramolecular coordination can be regarded as very strong (2.4590(19) Å). The N1–Sn1–N2 interatomic angle of 168.03(6)° slightly differs from the ideal flat angle probably due to the sterical hindrance of the two phenyl substituents. The azide unit is nearly linear (178.0(2)°) but bent at the nitrogen atom, with Sn–N2–N3 interatomic angle of 111.22(14)°.

Generally, the bonding in the $\text{M}-\text{N}_3$ species may be described by two main canonical forms: $\text{M}-\text{N}=\text{N}=\text{N}$ and $\text{M}-\text{N}-\text{N}\equiv\text{N}$. In addition, an ionic resonance form $\text{M}^+[\text{N}_3]^-$ may also contribute to a certain degree to the overall bonding pattern.^{11,12,38} The structural data of **2** suggest that based on the covalent radii³⁹ of nitrogen atoms there is no dominant canonical form of the Sn-azide moiety (N2–N3 = 1.194(3) Å, N3–N4 = 1.150(3) Å). This bonding pattern is also consistent with the results obtained from the theoretical calculations.¹²

Two non-equivalent (axial and equatorial) azide moieties can be found in the molecular structure of **4** in which the tin atom is again five-coordinated with heavily distorted trigonal bipyramidal geometry (Fig. 3). Owing to the presence of the two mentioned azide units, the intramolecular N→Sn coordination is even stronger (Sn1–N1 = 2.410(2) Å) than in the case of **2**. The N1–Sn1–N2 interatomic angle of 169.83(8)° differs only subtly from the ideal flat angle. The Sn1–N2 bond (2.183(2) Å) is noticeably longer than the Sn1–N5 bond (2.114(2) Å) due to the *trans*-effect of the donor pendant arm of the C,N-chelating ligand. Again, there is no dominant canonical form of the Sn-azide moiety (N2–N3 = 1.198(3) Å and N3–N4 = 1.147(3) Å; N5–N6 = 1.205(4) Å and N6–N7 = 1.145(4) Å, respectively). Both azide substituents are almost linear (175.6(3)° and 176.3(3)°) and again bent at the nitrogen N2 and N5 (Sn1–N2–N3 = 119.87(19)° and Sn1–N5–N6 = 120.7(2)°, respectively). A detailed investigation of the crystal packing in **4** revealed the presence of intermolecular N→Sn (3.278 Å, $\sum r_{\text{vdw}}(\text{Sn}, \text{N}) \approx 3.9$ Å)⁴⁰ and N⋯H–C (3.285 Å, 122.74°) short contacts resulting from the interaction of the equatorial azide moiety from one molecule



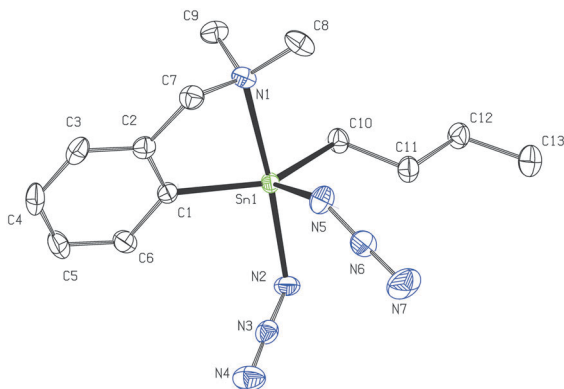


Fig. 3 Molecular structure of **4** (ORTEP presentation, 50% probability level). Hydrogen atoms are omitted for clarity. Selected interatomic distances [Å] and angles [°]: Sn1–N1 2.410(2), Sn1–N2 2.183(2), Sn1–N5 2.114(2), N2–N3 1.198(3), N3–N4 1.147(3), N5–N6 1.205(4), N6–N7 1.145(4), Sn1–C1 2.116(3), Sn1–C10 2.126(3); N1–Sn1–N2 169.83(8), Sn1–N2–N3 119.87(19), Sn1–N5–N6 120.7(2), N2–N3–N4 176.3(3), N5–N6–N7 175.6(3), C1–Sn1–C10 144.16(10), C1–Sn1–N5 104.74(9), C10–Sn1–N5 108.65(9).

with the tin atom and the *n*-Bu substituent of the second molecule giving rise to an infinite chain (Fig. S1, ESI†).

The tin atom in monomeric **6** is octahedrally coordinated as a result of the C,N-chelate bonding of two L^{CN} groups and two *cis*-bonded azide units (Fig. 4). The C1 and C10 atoms are mutually in *trans* positions, while the intramolecularly coordinated nitrogen atoms are bonded in a *cis* fashion. The main deviation from the ideal octahedral geometry is the C1–Sn1–C10 (157.22(11)° vs. ideal 180°) angle. The interatomic distances Sn1–N1 (2.487(3) Å) and Sn1–N2 (2.606(3) Å) mutually differ but are still within the range expected for intramolecular N→Sn interactions. In **6** each nitrogen of the ligand pendant arm is disposed *trans* to one azide moiety (N1–Sn1–N3 = 164.64(11)° and N2–Sn1–N6 = 169.32(12)°). Both azide units exhibit nearly ideal linear

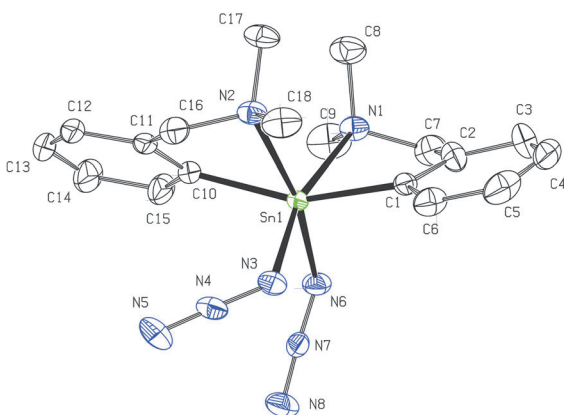


Fig. 4 Molecular structure of **6** (ORTEP presentation, 40% probability level). Hydrogen atoms are omitted for clarity. Selected interatomic distances [Å] and angles [°]: Sn1–N1 2.487(3), Sn1–N2 2.606(3), Sn1–N3 2.178(3), Sn1–N6 2.165(3), N3–N4 1.205(5), N4–N5 1.140(6), N6–N7 1.197(4), N7–N8 1.149(5), Sn1–C1 2.112(3), Sn1–C10 2.129(4); N1–Sn1–N3 164.64(11), N2–Sn1–N6 169.32(12), Sn1–N3–N4 119.0(2), Sn1–N6–N7 120.7(3), C1–Sn1–C10 157.22(11), N3–N4–N5 176.2(4), N6–N7–N8 175.6(4).

arrangement (N3–N4–N5 = 176.2(4)° and N6–N7–N8 = 175.6(4)°, respectively) and, similarly to the situation described for all previous compounds, the Sn–N₃ fragments are bent at nitrogen (Sn1–N3–N4 = 119.0(2) and Sn1–N6–N7 = 120.7(3)°, respectively). No dominant canonical form can be described for the Sn-azide moiety in **6** (N3–N4 = 1.205(5) Å and N4–N5 = 1.140(6) Å; N6–N7 = 1.197(4) Å and N7–N8 = 1.149(5) Å, respectively), too.

From another point of view, the Sn–N₃ interatomic distance in **2** (2.2298(19) Å) is somewhat longer when compared to the values reported for the monomeric Ph₃SnN₃·HMPA (2.217(6) Å) and polymeric Ph₃SnN₃ (2.210(3) Å).^{4a} This phenomenon could be simply explained by the strong *trans*-effect of the pendant arm of the L^{CN} ligand.²¹ On the other hand, diorganotin(IV) bis(azides) **4** and **6** reveal much shorter tin-azide interatomic distances (up to 2.114(2) Å for **4** and 2.165(3) Å in the case of **6**). Such Sn–N₃ interatomic distances are comparable with those reported for both monomeric (e.g. (*t*-Bu)₂Sn(N₃)₂; 2.156(3) and 2.141(2) Å)⁷ and some polymeric organotin(IV) azides (e.g. Bn₃SnN₃; 2.16(1) Å).⁵

2.3.2 Molecular structures of 8, 10, 11 and 14a. Unambiguous differentiation of the crystalline organotin(IV) tetrazolide regioisomers was established by XRD techniques. As mentioned *vide supra* the incorporation of the relatively small CH₃CN fragment originating from the acetonitrile molecule within the heterocyclic ring provides the C,N-chelated dialkyl/aryltin(IV) 5-methyl-tetrazol-1-ide regioisomer of **8** (Fig. 5, Fig. S2 and S3, ESI†). Three independent molecules are present in the unit cell of **8**, where two of them are a part of 2-D networks interconnected by solvating water molecules and the remaining one interacts *via* a non-covalent contact with the chloroform molecule only (Fig. S3, ESI†).

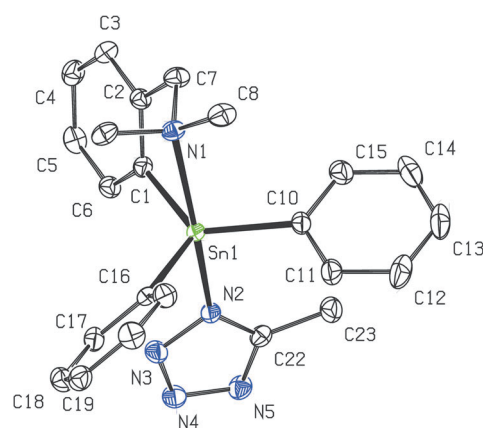


Fig. 5 Molecular structure of **8** (ORTEP presentation, 40% probability level). Solvating CHCl₃ and water molecules as well as all hydrogen atoms are omitted for clarity. Selected interatomic distances [Å] and angles [°]; only selected parameters of one representative molecule are shown, the rest of them is presented in Fig. S2 (ESI†): Sn1–N1 2.466(5), Sn1–N2 2.263(5), N2–N3 1.361(6), N3–N4 1.302(7), N4–N5 1.358(6), N2–C22 1.344(7), N5–C22 1.315(8), Sn1–C1 2.126(5), Sn1–C10 2.126(5), Sn1–C16 2.132(5); N1–Sn1–N2 169.33(13), Sn1–N2–N3 116.7(3), N2–N3–N4 108.5(4), N3–N4–N5 109.6(4), N4–N5–C22 105.8(4), N2–C22–N5 110.8(4), C22–N2–N3 105.4(4), C1–Sn1–C10 122.89(18), C1–Sn1–C16 123.09(18), C10–Sn1–C16 112.57(19).



The vicinity of the central tin atom with distorted trigonal bipyramidal geometry in **8** is preserved which is in accordance with the ^{119}Sn NMR studies. The average intramolecular $\text{N} \rightarrow \text{Sn}$ interaction of *ca.* 2.46 Å is very strong and comparable with that discussed for **2** (2.459(19) Å). The average axial $\text{N}-\text{Sn}-\text{N}$ interatomic angle of *ca.* 169.3° is even closer to the ideal 180° than in **2** (168.03(6)). The CN_4 tetrazolide ring is planar with a maximum torsion angle of 1° among all atoms. All interatomic distances in the CN_4 tetrazolide ring exhibit reasonable values (see the caption of Fig. 5) that were described for such heterocyclic systems.^{39,41} On the other hand, it is evident that at least partial π -electron delocalization must be considered due to the decrease of differences between formal $\text{N}-\text{N}$, $\text{N}=\text{N}$, $\text{C}-\text{N}$ and $\text{C}=\text{N}$ bond lengths^{39,41} or when compared to the interatomic distances reported for other organotin(IV) tetrazolides.^{19b,c}

Contrary to **8**, the bulky *t*-butyl substituent requires the formation of C,N-chelated dialkyl/aryl tin(IV) 5-*t*-butyltetrazol-2-ide regioisomers **9** and **10**. The vicinity of the central tin atom in **10** adopts the same geometry as in the case of **8** with a slightly weaker intramolecular $\text{N} \rightarrow \text{Sn}$ coordination (2.522(2) Å; Fig. 6). Surprisingly, all nitrogen–nitrogen and carbon–nitrogen interatomic distances in the planar tetrazolide ring are mutually even closer (ranging from 1.321 to 1.345 Å) which suggests a higher degree of π -electron delocalization. Essentially the same trend was found for the molecular structure of **11** (Fig. 7), which bears two *n*-Bu substituents on the central five-coordinated tin atom. All other interatomic distances and angles lie within the usual range for this class of compounds. In the case of **11**, the Ph substituent is nearly co-planar with the N_4C ring (maximum torsion angle of 4.8°).

Finally, several single crystals of free 5-*N,N*-dimethylamino-methyl-1*H*-tetrazole **14a** (Fig. S4 and S5, ESI†) were obtained

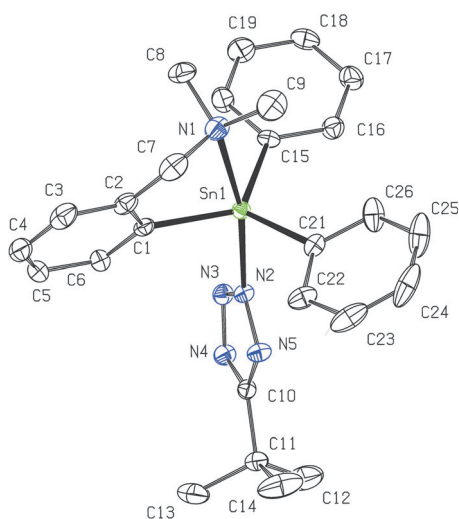


Fig. 6 Molecular structure of **10** (ORTEP presentation, 40% probability level). Hydrogen atoms are omitted for clarity. Selected interatomic distances [Å] and angles [°]: $\text{Sn1}-\text{N1}$ 2.522(2), $\text{Sn1}-\text{N2}$ 2.2218(19), $\text{N2}-\text{N3}$ 1.321(3), $\text{N3}-\text{N4}$ 1.331(3), $\text{N2}-\text{N5}$ 1.343(3), $\text{N4}-\text{C10}$ 1.345(3), $\text{N5}-\text{C10}$ 1.329(3), $\text{Sn1}-\text{C1}$ 2.123(2), $\text{Sn1}-\text{C15}$ 2.126(2), $\text{Sn1}-\text{C21}$ 2.119(2); $\text{N1}-\text{Sn1}-\text{N2}$ 167.50(7), $\text{Sn1}-\text{N2}-\text{N3}$ 126.52(15), $\text{N2}-\text{N3}-\text{N4}$ 107.59(18), $\text{N3}-\text{N2}-\text{N5}$ 111.43(18), $\text{N3}-\text{N4}-\text{C10}$ 105.82(18), $\text{N2}-\text{N5}-\text{C10}$ 103.41(18), $\text{C1}-\text{Sn1}-\text{C15}$ 123.10(8), $\text{C1}-\text{Sn1}-\text{C21}$ 117.80(9), $\text{C15}-\text{Sn1}-\text{C21}$ 116.66(9).

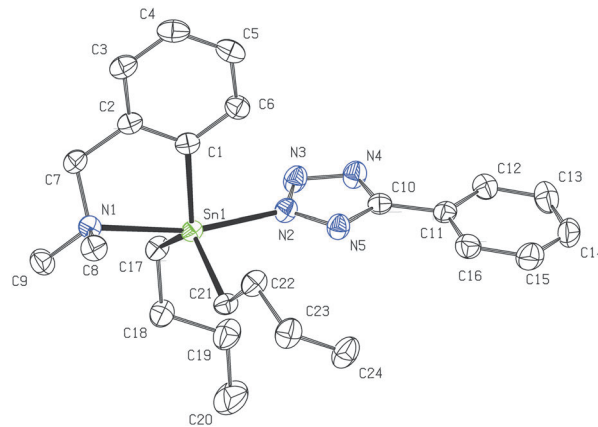


Fig. 7 Molecular structure of **11** (ORTEP presentation, 50% probability level). Hydrogen atoms are omitted for clarity. Selected interatomic distances [Å] and angles [°]: $\text{Sn1}-\text{N1}$ 2.480(2), $\text{Sn1}-\text{N2}$ 2.280(2), $\text{N2}-\text{N3}$ 1.319(3), $\text{N3}-\text{N4}$ 1.332(3), $\text{N2}-\text{N5}$ 1.344(3), $\text{N4}-\text{C10}$ 1.346(3), $\text{N5}-\text{C10}$ 1.332(3), $\text{Sn1}-\text{C1}$ 2.138(2), $\text{Sn1}-\text{C17}$ 2.144(2), $\text{Sn1}-\text{C21}$ 2.141(2); $\text{N1}-\text{Sn1}-\text{N2}$ 166.37(7), $\text{Sn1}-\text{N2}-\text{N3}$ 123.29(15), $\text{N2}-\text{N3}-\text{N4}$ 108.21(19), $\text{N3}-\text{N2}-\text{N5}$ 111.22(19), $\text{N3}-\text{N4}-\text{C10}$ 105.20(19), $\text{N2}-\text{N5}-\text{C10}$ 103.21(18), $\text{C1}-\text{Sn1}-\text{C17}$ 126.61(9), $\text{C1}-\text{Sn1}-\text{C21}$ 117.30(8), $\text{C17}-\text{Sn1}-\text{C21}$ 119.85(9).

upon unintentional acidolysis of **14**. It was found that **14a** crystallizes as a centrosymmetric dimer due to the H-bonding between the N1 and N5 atoms. In this particular case the mutual differences between interatomic distances are significantly larger than discussed for **10** and **11**, respectively.

2.4 Theoretical investigations

The formation of different regioisomers with respect to the substitution pattern of the nitrile reagent in the [3+2] cycloaddition reaction has prompted a theoretical study on selected compounds (**8**, **10**, **11**, **14**, **15** and **16**). The optimized geometries of all complexes (for more details see Fig. S6 and S7, ESI†) are in good agreement with the XRD data with a slightly underestimated intramolecular $\text{N} \rightarrow \text{Sn}$ interaction (*ca.* 7%, for comparison of the theoretical and experimental data see Table S5, ESI†).

The DFT calculations confirmed that for the complexes formed in the reaction of organotin(IV) azides with nitriles bearing either a small or a flexible substituent (**8** and **14**), the organotin(IV) 5-*R*-tetrazol-1-ide regioisomers are 0.4 (**8**) and 2.9 (**14**) kcal mol^{−1} lower in energy than the organotin(IV) 5-*R*-tetrazol-2-ide regioisomers. On the other hand, the organotin(IV) 5-*R*-tetrazol-2-ide regioisomers are predicted to be more stable when synthesized from nitriles with bulkier substituents (*t*-Bu and Ph for **10** and **11**, respectively) which again correlates very well with the experimental findings. The relatively small energy differences between the studied regioisomers suggest that the exclusive formation of only one regioisomer in all studied reactions is affected by the kinetic effects similarly as described in the previous studies.⁴² Alternatively, the regioselectivity of the studied reactions can be explained on the basis of the solid-state effects resulting in the crystallization of only one regioisomer from a solution where both isomers are present in a very rapid equilibrium.

Since the desired organotin(IV) triazolides were only formed in the reaction with cyclooctyne, the reactions of organotin(IV)



azides **1** and **2** with cyclooctyne and substituted acetylenes were examined (the energy and Gibbs free energy differences for all the studied cycloaddition reactions are collected in Table S4, ESI†). A mutual comparison of the ΔG values of the cycloaddition reactions reveals that the reactions of the organotin(IV) azides with the cyclic and acyclic alkynes are significantly more exergonic than the reactions with nitriles. Nevertheless, the previous studies showed that a high activation barrier kinetically hinders the formation of the respective triazolide complexes.^{17b} Therefore, the higher reaction rate of cyclooctyne can be explained by the bond angle deformation to *ca.* 160°, which is distorted toward the transition state of the cycloaddition reaction, resulting in a dramatic rate acceleration.⁴³

3. Conclusion

We have expanded the family of known C,N-chelated organotin(IV) pseudohalides by the introduction of the azide substituent(s). The possible use of these compounds within the click chemistry (*i.e.* preparation of various organotin(IV) triazolides and tetrazolides) has been successfully authenticated. In addition, the C,N-chelated triorganotin(IV) azides **1** and **2** may be utilized as mild azidation reagents in the synthetic chemistry. Furthermore, C,N-chelated organotin(IV) azides may be used for bioorthogonal labeling of biologically active species. Finally, tri- and tetrazolides can serve as a source of heterocycles by simple protonolysis or *via* conversion with E-Cl bond(s) analogously to our fluorination agents described earlier.⁴⁴

All mentioned species are monomeric both in solution and in the solid state. Theoretical calculations proved the regioselectivity of the formation of the respective tetrazolides as well as a higher activation barrier of the reactions of azides with acetylenes.

4. Experimental section

4.1 General remarks

All reactions were carried out in the air unless stated otherwise. All reagents and solvents were obtained from commercial sources (Sigma-Aldrich). **Caution!** Sodium azide is extremely toxic. Handle with care! $L^{CN}(n\text{-Bu})_2\text{SnCl}$,²² $L^{CN}\text{Ph}_2\text{SnCl}$,^{23,25b} $(L^{CN})_2(n\text{-Bu})\text{SnCl}$,²² $L^{CN}(n\text{-Bu})\text{SnCl}_2$,²² $L^{CN}\text{PhSnCl}_2$,²⁴ $(L^{CN})_2\text{SnBr}_2$ ²⁴ and cyclooctyne⁴⁵ were prepared according to published procedures.

4.2 NMR spectroscopy

The NMR spectra were recorded from solutions in C_6D_6 , THF- d_8 and CDCl_3 on a Bruker Ascend™ 500 spectrometer (equipped with a Z-gradient 5 mm Prodigy cryoprobe) at frequencies ^1H (500.13 MHz), $^{13}\text{C}\{^1\text{H}\}$ (125.76 MHz) and $^{119}\text{Sn}\{^1\text{H}\}$ (186.50 MHz) at 295 K. The solutions were obtained by dissolving approximately 40–60 mg of each compound in 0.6 mL of deuterated solvent. The values of ^1H chemical shifts were calibrated to residual signals of CDCl_3 ($\delta(^1\text{H}) = 7.27$ ppm), C_6D_6 ($\delta(^1\text{H}) = 7.16$ ppm) or THF- d_8 ($\delta(^1\text{H}) = 3.58$ ppm). The values of ^{13}C chemical shifts were calibrated to signals of CDCl_3 ($\delta(^{13}\text{C}) = 77.2$ ppm), C_6D_6 ($\delta(^{13}\text{C}) = 128.39$ ppm) or THF- d_8 ($\delta(^{13}\text{C}) = 67.57$ ppm). The ^{119}Sn

chemical shift values are referenced to external neat tetramethyl stannane ($\delta(^{119}\text{Sn}) = 0.0$ ppm). Positive chemical shift values denote shifts to the higher frequencies relative to the standards.

4.3 Crystallography

The X-ray data (Tables S2 and S3, ESI†) for colourless crystals of **2**, **4**, **6**, **8**, **10**, **11** and **14a** were obtained at 150 K using an Oxford Cryostream low-temperature device on a Nonius KappaCCD diffractometer with MoK_α radiation ($\lambda = 0.71073$ Å), a graphite monochromator in ϕ and χ scan modes. Data reductions were performed using DENZO-SMN.⁴⁶ The absorption was corrected by integration methods.⁴⁷ Structures were solved by direct methods (Sir92)⁴⁸ and refined by full matrix least-square based on F^2 (SHELXL-97).⁴⁹ Hydrogen atoms were mostly localized on a difference Fourier map, however to ensure uniformity of the treatment of the crystal, all hydrogen atoms were recalculated into idealized positions (riding model) and assigned temperature factors $H_{\text{iso}}(\text{H}) = 1.2U_{\text{eq}}$ (pivot atom) or of $1.5U_{\text{eq}}$ for the methyl moiety with C–H = 0.96, 0.97, and 0.93 Å for methyl, methylene and hydrogen atoms in aromatic rings, respectively, and 0.82 Å for N–H groups. The dynamic disorder of the co-crystallized solvent (CHCl_3) in the structure of **8** was treated by standard methods.⁴⁹

4.4 ESI MS analysis

The MS spectra were measured on a Bruker MicroTOF-QIII apparatus using the ESI source in the positive mode. The measurement parameters were adjusted as follows: the capillary voltage was 4200 V and the end plate offset was –500 V. The collision cell RF was 350 V_{pp} . The nebulizer gas (N_2) pressure was 1.6 bar and the flow of drying gas (N_2 , heated to 180 °C) was 8 l min^{-1} . Scans of MS spectra were carried out in the mass range of m/z 80–1550. For the HRMS measurements, the calibration on sodium formate clusters was used. The samples were delivered by direct infusion using a syringe pump (Kd-Scientific, KDS-100-CE, 0.5 mL Hamilton syringe, flow rate 180 $\mu\text{L min}^{-1}$) coupled to the MicroTOF-QIII mass spectrometer. For the MS/MS measurements, the precursor ions were isolated by the collision cell energy of 2 eV in the window of $2u$ and the product ions were obtained with collision cell energy increasing from 15 to 40 eV, depending on the compound studied.

4.5 IR spectroscopy

The IR spectra of neat samples were recorded on a Bruker Vector 22 FT-IR spectrometer using the ATR method at ambient temperature.

4.6 DFT calculations

All calculations were carried out using Density Functional Theory (DFT) as implemented in the Gaussian09 quantum chemistry program.⁵⁰ Geometry optimizations were carried out at the M06/cc-pVDZ(cc-pVDZ-pp for Sn) level of theory and the energies of the optimized structures were re-evaluated by additional single point calculations on each of all optimized geometries using the triple- ζ -quality cc-pVTZ-pp basis set.⁵¹ Analytical vibrational



frequencies within the harmonic approximation were computed using the cc-pVDZ basis set to confirm appropriate convergence to well-defined minima or saddle points on the potential energy surface. The Gibbs free energies $G^{\text{solv}}(\text{cc-pVTZ})$ used to calculate the energy differences reported in this article (Table S4, ESI†) have been computed with the following protocol:

$$G^{\text{solv}}(\text{cc-pVTZ}) = G(\text{cc-pVTZ}) + \text{SC} \quad (1)$$

$$G(\text{cc-pVTZ}) = E(\text{cc-pVTZ}) + \text{TC} \quad (2)$$

$$\text{TC} = G(\text{cc-pVDZ}) - E(\text{cc-pVDZ}) \quad (3)$$

$$\text{SC} = E^{\text{solv}}(\text{cc-pVDZ}) - E(\text{cc-pVDZ}) \quad (4)$$

$E(x)$ is the self-consistent field energy in the cc-pVDZ or cc-pVTZ basis sets respectively and TC is the thermal correction to the energy calculated for the cc-pVDZ basis set. $G(\text{cc-pVDZ})$ is the free energy at 298.15 K for the double- ζ -quality basis set. SC is the solvent correction calculated using $E^{\text{solv}}(\text{cc-pVDZ})$, which is the self-consistent field energy in the SMD implicit solvation model using chloroform as solvent ($\epsilon = 4.71$) in the cc-pVDZ basis set.⁵²

4.7 Synthesis

The general procedure for the synthesis of **1–16** is described. For details concerning both synthesis and spectroscopic characterization of all compounds see the ESI.†

4.7.1 General procedure for the preparation of 1–6. Starting C,N-chelated organotin(IV) halide (usually 1.0 mmol) was dissolved in diethyl ether or dichloromethane (*ca.* 10–15 mL). Sodium azide (usually 5.0 mmol) in water (*ca.* 10 mL) was then added and the final biphasic reaction mixture was stirred overnight. Afterwards, the water phase was separated and washed with diethyl ether or dichloromethane (2×10 mL). The combined organic phases were dried over MgSO_4 . After filtration, the clear solution of the respective product was evaporated to dryness *in vacuo* giving **1–6** as crystalline solids or yellowish oils in yields up to 85%.

4.7.2 General procedure for the preparation of 7–16

Method A. Starting C,N-chelated organotin(IV) azide **1** or **2** was heated to reflux for the required period of time with an excess of organic nitrile in toluene giving pure **7–14** after evaporation of all volatiles *in vacuo*. Essentially quantitative yields of the desired products were obtained.

Method B. Starting C,N-chelated organotin(IV) azide **1** or **2** and a stoichiometric amount of organic nitrile or cyclooctyne were sealed under vacuum in the NMR tube in benzene- d_6 . Afterwards, the NMR tube was heated to 100 °C for a required period of time to achieve a complete conversion towards the desired products (**11–16**) of the [3+2] cycloaddition. Quantitative yields of the respective products were obtained.

Acknowledgements

The authors would like to thank the Czech Science Foundation for the financial support of this work (project P207/12/0223).

J. T. would like to acknowledge the financial support of FWO, under the scheme FWO Pegasus Marie Curie fellowship (Project No. 12T6615N). F. D. P. wishes to acknowledge the Free University of Brussels (VUB) and the Research Foundation Flanders (FWO) for continuous support to his group.

References

- (a) J. G. A. Luijten, M. J. Janssen and G. J. M. van der Kerk, *Recl. Trav. Chim. Pays-Bas*, 1962, **81**, 202; (b) J. S. Thayer and R. West, *Inorg. Chem.*, 1964, **3**, 406.
- J. Lorberth, H. Krapf and H. Noth, *Chem. Ber.*, 1967, **100**, 3511.
- R. Allmann, R. Hohlfeld, A. Waskowska and J. Lorberth, *J. Organomet. Chem.*, 1980, **192**, 353.
- (a) I. Wharf, R. Wojtowski, C. Bowes, A.-M. Lebius and M. Onyschuk, *Can. J. Chem.*, 1998, **76**, 1827; (b) R. Campbell, M. F. Davis, M. Fazakerley and P. Portius, *Chem. – Eur. J.*, 2015, **21**, 1.
- A. C. Burke, M. F. Mahon and K. C. Molloy, *Appl. Organomet. Chem.*, 2003, **17**, 735.
- R. A. Howie, J. L. Wardell and S. M. S. V. Wardell, *Appl. Organomet. Chem.*, 2005, **19**, 356.
- D. Hänssgen, M. Jansen, C. Leben and T. Oster, *J. Organomet. Chem.*, 1995, **494**, 223.
- J. A. S. Bomfim, C. A. L. Filgueiras, R. A. Howie, J. N. Low, J. M. S. Skakle, J. L. Wardell and S. M. S. V. Wardell, *Polyhedron*, 2002, **21**, 1667.
- (a) A. M. Khmaruk and A. M. Pinchuk, *Zh. Org. Khim.*, 1983, **19**, 883; (b) P. B. Hitchcock, M. F. Lappert, A. V. Protchenko and P. G. H. Uiterweerd, *Dalton Trans.*, 2009, 353; (c) P. Švec, Z. Padělková, M. Alonso, F. De Proft and A. Růžicka, *Can. J. Chem.*, 2014, **92**, 434.
- M. S. Nechaev, *THEOCHEM*, 2008, **862**, 49.
- A. E. Ayers, T. M. Klapötke and H. V. R. Dias, *Inorg. Chem.*, 2001, **40**, 1000.
- A. E. Ayers, D. S. Marynick and H. V. R. Dias, *Inorg. Chem.*, 2000, **39**, 4147.
- H. V. R. Dias and A. E. Ayers, *Polyhedron*, 2002, **21**, 611.
- H. C. Kolb, M. G. Finn and K. B. Sharpless, *Angew. Chem., Int. Ed.*, 2001, **40**, 2004.
- For example see: (a) M. G. Finn and V. V. Fokin, *Chem. Soc. Rev.*, 2010, **39**, 1231; (b) R. A. Evans, *Aust. J. Chem.*, 2007, **60**, 384; (c) P. L. Golas and K. Matyjaszewski, *Chem. Soc. Rev.*, 2010, **39**, 1338; (d) Y. Hua and A. H. Flood, *Chem. Soc. Rev.*, 2010, **39**, 1262; (e) N. J. Agard, J. A. Prescher and C. R. Bertozzi, *J. Am. Chem. Soc.*, 2004, **126**, 15046; (f) Z. P. Demko and K. B. Sharpless, *Org. Lett.*, 2001, **3**, 4091.
- (a) R. Huisgen, *Proc. Chem. Soc., London*, 1961, 357; (b) R. Huisgen, *Angew. Chem., Int. Ed.*, 1963, **2**, 565.
- (a) C. G. Gordon, J. L. Mackey, J. C. Jewett, E. M. Sletten, K. N. Houk and C. R. Bertozzi, *J. Am. Chem. Soc.*, 2012, **134**, 9199; (b) F. Schoenebeck, D. H. Ess, G. O. Jones and K. N. Houk, *J. Am. Chem. Soc.*, 2009, **131**, 8121.



- 18 K. Sisido, K. Nabika and T. Isida, *J. Organomet. Chem.*, 1971, **33**, 337.
- 19 (a) M. F. Mahon, K. C. Molloy and P. C. Waterfield, *J. Organomet. Chem.*, 1989, **361**, C5; (b) S. J. Blunden, M. F. Mahon, K. C. Molloy and P. C. Waterfield, *J. Chem. Soc., Dalton Trans.*, 1994, 2135; (c) M. Hill, M. F. Mahon and K. C. Molloy, *J. Chem. Soc., Dalton Trans.*, 1996, 1857; (d) M. Hill, M. F. Mahon, J. McGinley and K. C. Molloy, *J. Chem. Soc., Dalton Trans.*, 1996, 835; (e) A. Goodger, M. Hill, M. F. Mahon, J. McGinley and K. C. Molloy, *J. Chem. Soc., Dalton Trans.*, 1996, 847.
- 20 (a) G. van Koten, C. A. Schaap and J. G. Noltes, *J. Organomet. Chem.*, 1975, **99**, 157; (b) G. van Koten, J. G. Noltes and A. L. Spek, *J. Organomet. Chem.*, 1976, **118**, 183; (c) G. van Koten, J. T. B. H. Jastrzebski, J. G. Noltes, A. L. Spek and J. C. Schoone, *J. Organomet. Chem.*, 1978, **148**, 233.
- 21 J. T. B. H. Jastrzebski and G. van Koten, *Adv. Organomet. Chem.*, 1993, **35**, 241.
- 22 A. Růžicka, V. Pejchal, J. Holeček, A. Lyčka and K. Jacob, *Collect. Czech. Chem. Commun.*, 1998, **63**, 977.
- 23 A. Růžicka, R. Jambor, J. Brus, I. Císařová and J. Holeček, *Inorg. Chim. Acta*, 2001, **323**, 163.
- 24 P. Novák, Z. Padělková, L. Kolářová, I. Císařová, A. Růžicka and J. Holeček, *Appl. Organomet. Chem.*, 2005, **19**, 1101.
- 25 (a) R. A. Varga, A. Rotar, M. Schurmann, K. Jurkschat and C. Silvestru, *Eur. J. Inorg. Chem.*, 2006, 1475; (b) R. A. Varga, M. Schurmann and C. Silvestru, *J. Organomet. Chem.*, 2001, **623**, 161; (c) A. Rotar, R. A. Varga, K. Jurkschat and C. Silvestru, *J. Organomet. Chem.*, 2009, **694**, 1385; (d) R. A. Varga, K. Jurkschat and C. Silvestru, *Eur. J. Inorg. Chem.*, 2008, 708.
- 26 (a) P. Novák, J. Brus, I. Císařová, A. Růžicka and J. Holeček, *J. Fluorine Chem.*, 2005, **126**, 1531; (b) P. Novák, Z. Padělková, I. Císařová, L. Kolářová, A. Růžicka and J. Holeček, *Appl. Organomet. Chem.*, 2006, **20**, 226.
- 27 C. Coza, A. Stegarescu, R. Șuteu and A. Silvestru, *J. Organomet. Chem.*, 2015, 777, 71.
- 28 P. Švec, Z. Růžicková, P. Vlasák, J. Turek, F. De Proft and A. Růžicka, *J. Organomet. Chem.*, 2016, **801**, 14.
- 29 (a) L. Jin, D. R. Tolentino, M. Melaimi and G. Bertrand, *Sci. Adv.*, 2015, **1**, e1500304; (b) V. V. Rostovtsev, L. G. Green, V. V. Fokin and K. B. Sharpless, *Angew. Chem., Int. Ed.*, 2002, **41**, 2596.
- 30 (a) R. Huisgen, in *1,3-Dipolar Cycloaddition Chemistry*, ed. A. Padwa, Wiley, New York, 1984, pp. 1–176; (b) K. V. Gothelf and K. A. Jorgensen, *Chem. Rev.*, 1998, **98**, 863.
- 31 J. Turek, I. Panov, P. Švec, Z. Růžicková and A. Růžicka, *Dalton Trans.*, 2014, **43**, 15465.
- 32 J.-M. Vandensavel, G. Smets and G. L'abbé, *J. Org. Chem.*, 1973, **38**, 675.
- 33 (a) P. Švec, Z. Padělková, P. Štěpnička, A. Růžicka and J. Holeček, *J. Organomet. Chem.*, 2011, **696**, 1809; (b) P. Švec, E. Černošková, Z. Padělková, A. Růžicka and J. Holeček, *J. Organomet. Chem.*, 2010, **695**, 2475; (c) P. Švec, Z. Padělková, A. Růžicka, T. Weidlich, L. Dušek and L. Plasseraud, *J. Organomet. Chem.*, 2011, **696**, 676; (d) P. Švec, E. Černošková, Z. Padělková, A. Růžicka and J. Holeček, *J. Organomet. Chem.*, 2010, **695**, 2475; (e) P. Švec, R. Olejník, Z. Padělková, A. Růžicka and L. Plasseraud, *J. Organomet. Chem.*, 2012, **708**, 82.
- 34 (a) C. J. Pouchert and J. Behnke, *The Aldrich Library of ¹³C and ¹H FT NMR Spectra*, Aldrich Chemical Company, Inc., USA, 1993, vol. 1; (b) H. J. Reich, online NMR database accessible free of charge at <http://www.chem.wisc.edu/areas/organic/index-chem.htm>.
- 35 (a) G. Socrates, *Infrared Characteristic Group Frequencies*, John Wiley & Sons, Chichester, UK, 1980; (b) K. Nakamoto, *Infrared and Raman Spectra of Inorganic and Coordination Compounds*, John Wiley & Sons, New York, USA, 3rd edn, 1978.
- 36 (a) M. Holčapek, L. Kolářová, A. Růžicka, R. Jambor and P. Jandera, *Anal. Chem.*, 2006, **78**, 4210; (b) L. Kolářová, M. Holčapek, R. Jambor, L. Dostál, M. Nádvorník and A. Růžicka, *J. Mass Spectrom.*, 2004, **39**, 621.
- 37 H. A. Bent, *J. Chem. Phys.*, 1959, **33**, 1258.
- 38 V. N. Khrustalev, I. A. Portnyagin, N. N. Zemlyansky, I. V. Borisova, Y. A. Ustynyuk and M. Y. Antipin, *J. Organomet. Chem.*, 2005, **690**, 1056.
- 39 (a) P. Pykkö and M. Atsumi, *Chem. – Eur. J.*, 2009, **15**, 186; (b) P. Pykkö and M. Atsumi, *Chem. – Eur. J.*, 2009, **15**, 12770.
- 40 (a) A. Bondi, *J. Phys. Chem.*, 1964, **68**, 441; (b) B. Cordero, V. Gómez, A. E. Platero-Prats, M. Revés, J. Echeverría, E. Cremades, F. Barragán and S. Alvarez, *Dalton Trans.*, 2013, **42**, 8617.
- 41 F. H. Allen, O. Kennard, D. G. Watson, L. Brammer, A. G. Orpen and R. Taylor, *J. Chem. Soc., Perkin Trans. 2*, 1987, S1.
- 42 F. Himo, Z. P. Demko, L. Noodleman and K. B. Sharpless, *J. Am. Chem. Soc.*, 2002, **124**, 12210.
- 43 (a) R. Turner, A. D. Jarrett, P. Goebel and B. J. Mallon, *J. Am. Chem. Soc.*, 1972, **95**, 790; (b) K. Shea and J. S. Kim, *J. Am. Chem. Soc.*, 1992, **114**, 4846.
- 44 (a) P. Švec and A. Růžicka, *Main Group Met. Chem.*, 2011, **34**, 7; (b) P. Švec, A. Eisner, L. Kolářová, T. Weidlich, V. Pejchal and A. Růžicka, *Tetrahedron Lett.*, 2008, **49**, 6320.
- 45 L. Brandsma and H. D. Verkuijsse, *Synthesis*, 1978, 290.
- 46 Z. Otwinowski and W. Minor, *Methods Enzymol.*, 1997, **276**, 307.
- 47 P. Coppens, in *Crystallographic Computing*, ed. F. R. Ahmed, S. R. Hall and C. P. Huber, Copenhagen, Munksgaard, Denmark, 1970, pp. 255–270.
- 48 A. Altomare, G. Cascarano, C. Giacovazzo and A. Guagliardi, *J. Appl. Crystallogr.*, 1993, **26**, 343.
- 49 G. M. Sheldrick, *SHELXL-97*, University of Göttingen, Göttingen, Germany, 1997.
- 50 M. J. Frisch, G. W. Trucks, H. B. Schlegel, G. E. Scuseria, M. A. Robb, J. R. Cheeseman, G. Scalmani, V. Barone, B. Mennucci, G. A. Petersson, H. Nakatsuji, M. Caricato, X. Li, H. P. Hratchian, A. F. Izmaylov, J. Bloino, G. Zheng, J. L. Sonnenberg, M. Hada, M. Ehara, K. Toyota, R. Fukuda, J. Hasegawa, M. Ishida, T. Nakajima, Y. Honda, O. Kitao,



- H. Nakai, T. Vreven, J. A. Montgomery, Jr., J. E. Peralta, F. Ogliaro, M. Bearpark, J. J. Heyd, E. Brothers, K. N. Kudin, V. N. Staroverov, R. Kobayashi, J. Normand, K. Raghavachari, A. Rendell, J. C. Burant, S. S. Iyengar, J. Tomasi, M. Cossi, N. Rega, J. M. Millam, M. Klene, J. E. Knox, J. B. Cross, V. Bakken, C. Adamo, J. Jaramillo, R. Gomperts, R. E. Stratmann, O. Yazyev, A. J. Austin, R. Cammi, C. Pomelli, J. W. Ochterski, R. L. Martin, K. Morokuma, V. G. Zakrzewski, G. A. Voth, P. Salvador, J. J. Dannenberg, S. Dapprich, A. D. Daniels, Ö. Farkas, J. B. Foresman, J. V. Ortiz, J. Cioslowski and D. J. Fox, *Gaussian 09, Revision B.01*, Gaussian, Inc., Wallingford CT, 2009.
- 51 (a) Y. Zhao and D. G. Truhlar, *Theor. Chem. Acc.*, 2008, **120**, 215; (b) T. H. Dunning Jr, *J. Chem. Phys.*, 1989, **90**, 1007; (c) K. A. Peterson, *J. Chem. Phys.*, 2003, **119**, 11099.
- 52 (a) J. Tomasi, B. Mennucci and R. Cammi, *Chem. Rev.*, 2005, **105**, 2999; (b) A. V. Marenich, C. J. Cramer and D. G. Truhlar, *J. Phys. Chem. B*, 2009, **113**, 6378.

